

## Modelling of non-inductive current generation upon superposition of vertical field on EC heated plasma in the LATE device

T. Maekawa, K. Kuroda, M. Wada, M. Uchida, H. Tanaka

*Graduate School of Energy Science, Kyoto University, Kyoto, Japan*

A toroidal current was generated in a number of experiments when a weak vertical field ( $B_v$ ) was superposed in EC-heated toroidal plasmas [1-4]. Furthermore closed flux surfaces were often formed via a rapid current increase in small aspect ratio devices [3, 4]. These results are important since realization of compact tokamak reactors depends on reduction or elimination of a central solenoid from the reactors.

In order to understand the current generation mechanism and the equilibrium characteristics of plasmas in the external field composed of  $B_v$  and the toroidal field  $B_t$ , non-inductive current generation experiments have been carried out in the Low Aspect ratio Torus Experiment (LATE) device using 2.45GHz, 2s microwaves of 1-2 kW [5 (P5.150 in this conference)]. After the microwave of 1.5 kW is injected into the steady external field of  $B_v=6.8$ G and  $B_t=480$ G (both at  $R=25$ cm), a plasma current is generated and quickly increases up to 920A (typically in  $\sim 0.5$ s), and then is kept steady for 1.5 s until the end of the microwave pulse. Figure 1 shows profiles of electron density ( $n_e$ ), temperature ( $T_e$ ), pressure ( $p_e$ ) and space potential ( $V_s$ ) measured with Langmuir probe at the steady phase. In this experiment a top panel ( $Z=30$ cm), a bottom panel ( $Z=-30$ cm), and an ion energy analyser just behind an arced fine mesh slit on the top panel were installed. The radial profiles of vertical current onto the bottom and top panels, and the ion collector are shown in Fig.1(c).

In this paper the experimental results are examined using the plasma fluid model and also particle models. Radial and vertical force balances are primal to the force balance in the toroidal direction. Therefore, the radial and vertical components of the force balance

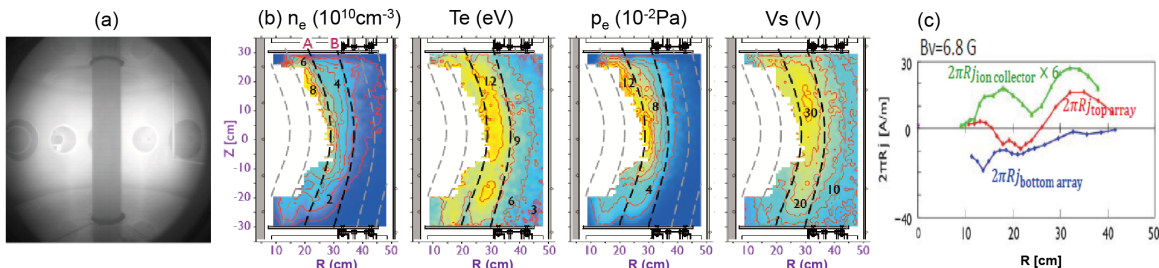


Fig.1 (a) Plasma image, (b) profiles of electron density, temperature, pressure and space potential, (c) radial current profiles onto the bottom and top panels and the ion collector during steady phase of discharge.  $R_{\text{ECR}}=13.8$ cm. The white area shows the probe tip locations where the interferometer line density along the chord  $R_t=12$ cm deteriorates by more than 10% compared with the values without probe insertion.

equation ( $\mathbf{j} \times \mathbf{B} = \nabla p$ ) and the condition of steady current circulation ( $\nabla \mathbf{j} = 0$ ) constitute the basic set of equations to analyse experimental results. Using  $R$  and  $Z$  components of  $\mathbf{j} \times \mathbf{B} = \nabla p$ , and  $\nabla \mathbf{j} = 0$ ,

$$\frac{\partial p}{\partial Z} = -j_\varphi B_R - \frac{R}{2} \left[ \frac{\partial(j_\varphi B_R)}{\partial R} + \frac{\partial(j_\varphi B_Z)}{\partial Z} \right]$$

The solution reads  $p(R, Z) = p_{VC}(R) + p_{TC}(R)$ , where

$$p_{TC}(R, Z) = \frac{R j_\varphi B_Z}{2} - \int^Z \left[ j_\varphi B_R + \frac{R}{2} \frac{\partial(j_\varphi B_R)}{\partial R} \right] dZ'$$

is related to the toroidal current  $j_\varphi$ , and  $p_{VC}(R)$  is responsible to the vertical current that circulates via the conducting vessel [6]. We may define  $p_{VC}$  as

$$p_{VC}(R) = \frac{R j_{VC} B_\varphi}{2},$$

where  $j_{VC}$  is the vertical current density.

Toroidal current profile is estimated from the magnetic analysis using 13 flux loops. First we employ a model of a single D-shaped area of toroidal current in which every local current has the same  $\varphi$  direction. The current smoothly becomes zero at the boundary and there is no current beyond the boundary. The model has 10 fitting parameters for ellipticity, triangularity, broadness or peaking factor for profile, shift of current peak position, location of D shape, etc. We search for a set of fitting parameters so that the flux values match to the measured flux values. Note that all the power supplies for toroidal and poloidal field coils are regulated with transistors and the noise levels on the flux loop signals are quite low. The best fit current profile for the plasma in Fig. 1 is shown in Fig. 2(a) with the fitting results to the flux loop signals in Fig. 2(b). No current exists near the bottom panel and this is

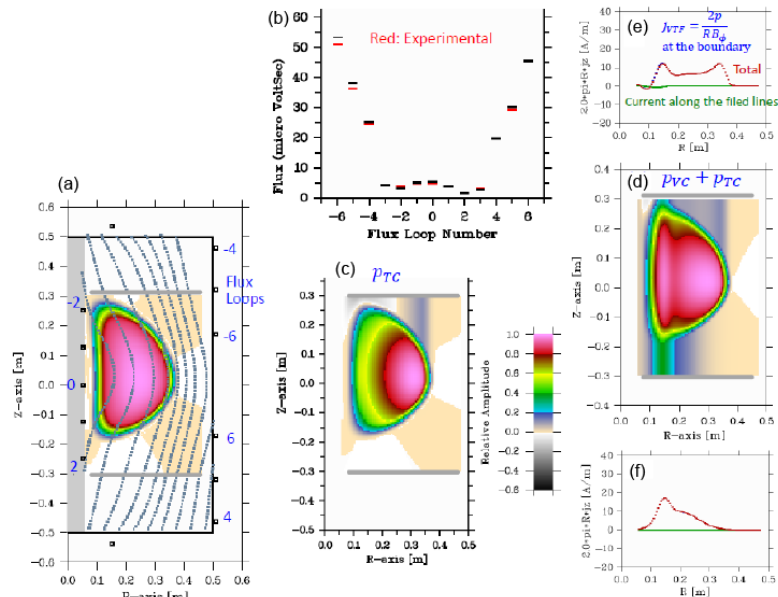


Fig. 2. Analysis with a single D-shape area of toroidal current. (a)  $j_\varphi$  and poloidal flux contours, (b) observed flux and fluxes from the model, (c)  $p_{TC}$  profile, (d)  $p_{TC} + p_{VC}$  profile, (e) and (f) radial profiles of current flowing onto the top panel and flowing out from the bottom panel, respectively.

the salient feature when we use this model. The pressure profile ascribed to the toroidal current is shown in Fig. 2(c). In order to match the vertical current through the bottom and top panels as well as its profile on the bottom panel to the experimental ones, we add an appropriate pressure profile ( $p_{VC}$ ) responsible to the vertical current. Sum of both pressures ( $p_{VC} + p_{TC}$ ) is shown in Fig. 2(d) with radial profiles of current flowing onto the top panel (Fig. 2(e)) and flowing out from the bottom panel (Fig. 2(f)). In this model parallel current along the field line is zero at the panel surfaces and therefore there is no contribution from the parallel current to the current onto the panels.

Next we take into account the contribution to  $j_\phi$  from the parallel currents that flow onto the top and bottom panels along the field lines as shown in Fig. 3(b). The total current profile and the fitting results to the flux loop signals are shown in Figs. 4(a) and 4(b), respectively. In order to match the vertical current through the bottom and top panels as well as its profile on the bottom panel to the experimental ones we add an appropriate pressure profile responsible to the vertical current. Figs. 4(e) and 4(f) show radial profiles of current flowing onto the top panel and flowing out from the bottom panel, respectively. Here the current onto the panels is contributed from the parallel current flowing along the field lines in addition to the vertical VTF drift current which is proportional to the edge pressure in front of the panels.

Comparison with the experimental results shows that the former model using a single current profile is not appropriate since the pressure profile near the

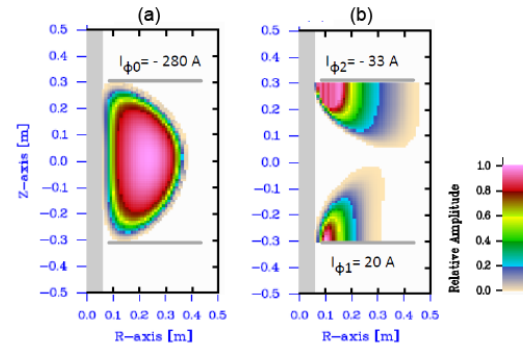


Fig.3. Profiles of (a) main toroidal current (b) toroidal components of the currents flowing onto the top and bottom panels along the field lines.

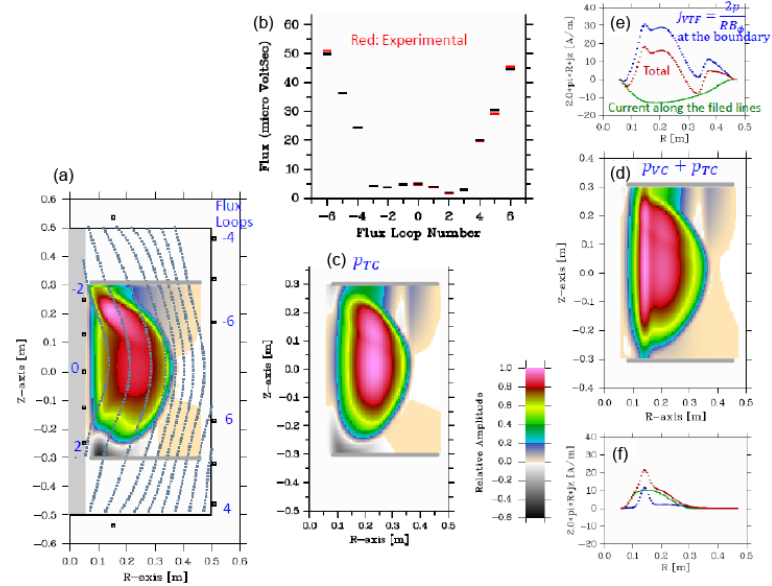


Fig. 4. Analysis by taking into account the contribution from the currents flowing onto the top and bottom panels along the field lines as those shown in Fig. 3. (a)  $j_\phi$  and poloidal flux contours, (b) observed flux and fluxes from the model, (c)  $p_{TC}$  profile, (d)  $p_{VC} + p_{TC}$  profile, (e) and (f) radial profiles of current flowing onto the top panel and flowing out from the bottom panel, respectively.

bottom panel does not match the experimental one (Fig. 1(c)), while the latter model fairly matches to the experimental profile. However, the absolute value of pressure is significantly larger than the experimental one, suggesting that contribution to pressure from the tail electrons is significant.

Even in the latter model the radial current profile onto the top panel does not match to the experimental one. This may show that fluid description for ion behavior fails near the top panel, where a steep potential slope onto the top panel exists as shown in Fig.1(b). Fig.5 shows typical ion orbits starting from the line from  $R=30\text{cm}$  to  $48\text{cm}$  at  $Z=20\text{cm}$ . The full orbits deviate from the guiding center orbits just before the top panel at inside of  $R<25\text{cm}$  corresponding to the fluid result in Fig.4(e). Note that the guiding center drift description is equivalent to the fluid description.

Using lots of full orbits of protons starting from the line  $R=30\text{cm}$  to  $48\text{cm}$  at  $Z=20\text{cm}$ , where the ions are assumed to have a Maxwell distribution with a temperature of  $T_i=2\text{eV}$  and the same density profile as the measured electron density profile, the ion behavior near the top panel is simulated. The simulated current profile onto the top panel ( $j_{\text{simulation}}$ ) matches to the current profile measured with the ion analyzer as shown in Fig.6.

### Acknowledgements

The present work was supported by KAKENHI (Grant Number 23360411 and 26289357).

### References

- [1] C. B. Forest et al., Phys. Rev. Lett 68 (1992) 3559.
- [2] V. Shevchenko et al., Proc. 25th Fusion Energy Conf., EX/P6-22 (2014)
- [3] T. Yoshinaga et al, Phys. Rev. Lett 96 (2006) 125005
- [4] M. Uchida et al, Nucl. Fusion 51 (2011) 063031
- [5] K. Kuroda, et al., 42nd EPS Conference on Plasma Phys. Lisbon, P5.150 (2015)
- [6] T. Maekawa, et al., Nucl. Fusion 52 (2012) 083008

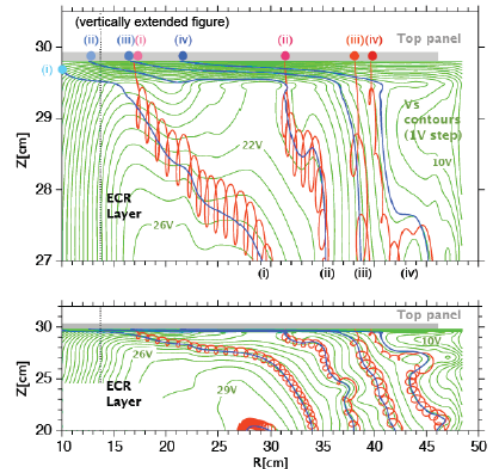


Fig.5. Full orbits (red) and the orbits using guiding center drift approximation (blue) starting from  $Z=20\text{cm}$  line with the initial kinetic energy of  $2\text{eV}$  and the pitch angle of  $63$  degrees. The upper figure is vertically extended to show the detail.

Fig.5 shows typical ion orbits starting from the line from  $R=30\text{cm}$  to  $48\text{cm}$  at  $Z=20\text{cm}$ . The full orbits deviate from the guiding center orbits just before the top panel at inside of  $R<25\text{cm}$  corresponding to the fluid result in Fig.4(e). Note that the guiding center drift description is equivalent to the fluid description.

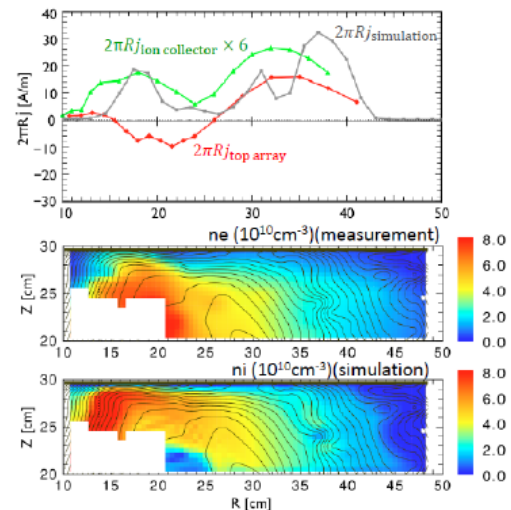


Fig.6. Comparison of experimental results and the results from full orbit analysis for ions.